Differential Beamformers Derived from Approximate Performance Measures

Conference Paper · September 2018

DOI: 10.1109/IWAENC.2018.8521409

4 authors:

Tao Long

Jacob Benesty
Institut National de la Recherche Scientifique

Jingdong Chen
Institute of Electrical and Electronics Engineers

Israel Cohen
Technion - Israel Institute of Technology

DIFFERENTIAL BEAMFORMERS DERIVED FROM APPROXIMATE PERFORMANCE MEASURES

Tao Long[1], *Jacob Benesty*[2], *Jingdong Chen*[1], *and Israel Cohen*[3]

[1]CIAIC and School of Marine Science and Technology, Northwestern Polytechnical University, Xi'an, Shaanxi, China, longtao@nwpu.edu.cn, jingdongchen@ieee.org
[2]INRS-EMT, University of Quebec, Montreal, Canada, benesty@emt.inrs.ca
[3]Department of Electrical Engineering, Technion - Israel Institute of Technology, Technion City, Haifa 32000, Israel, icohen@ee.technion.ac.il

ABSTRACT

Differential microphone arrays (DMAs) have attracted great interest over the past two decades, since this type of arrays can form frequency-invariant beampatterns and achieve maximum directional gains with a given number of sensors. Generally, the design of DMA beamformers involves optimization of some performance measures such as the directivity factor (DF), front-to-back ratio (FBR), white noise gain (WNG), etc. In this paper, we develop approximate performance measures, which basically approximate the integral part in the exact performance measures with a weighted sum. This approximation gets finer and finer as more points are used. When applied to the design of DMAs, the major advantages of using these approximate measures is that the design problem is simplified and many differential beamformers, including commonly-used standard ones, can be easily derived.

Index Terms— Differential microphone arrays, white noise gain, directivity factor, front-to-back ratio.

1. INTRODUCTION

Differential microphone arrays (DMAs) refer to arrays that are responsive to the spatial derivatives of the acoustic pressure field. DMAs have received an increasing research and development attention due to their wide range of applications in teleconferencing, hearing aids, robotics, smart home systems, etc [1, 2, 3, 4]. Traditionally, the design of differential beamformers are achieved by optimizing certain performance measures such as the DF, FBR, and WNG [5, 6, 7, 8, 9, 10, 11, 12]. Although a DMA has many attractive properties (such as frequency-invariant beampattern and high directional gain), its design is in general a nontrivial task especially for the higher-order one, since there are more parameters that need to be set during the design process.

In this paper, we develop two approximate performance measures for DMAs: the approximate DF and FBR. The basic idea is to approximate the integral part in the exact performance measures with some form of weighted summation. This approximation gets finer and finer as more points are used. The advantage of using these approximate performance measures is multifold. 1) These approximate measures are easy to evaluate. 2) Commonly-used differential beamformers can be easily derived. For example, we will show how to design beamformers with hypercardioid, supercardioid, cardioid, and dipole beampatterns. 3) Some new beamformers can be deduced, which are difficult to derive from the exact performance measures.

The work of T. Long was supported in part by the NSFC under grant 61601370 and 61425005. This work was also supported in part by Top International University Visiting Program for Outsanding Young scholars of Northwestern Polytechnical University, the Israel Science Foundation (grant no. 576/16) and the ISF-NSFC joint research program (grant No. 2514/17 and 61761146001).

2. SIGNAL MODEL AND PROBLEM FORMULATION

We consider the farfield case where a source of interest radiates an acoustic wave that propagates in an anechoic environment at the speed of sound, i.e., $c = 340$ m/s. The planar acoustic wave impinges on a uniform linear microphone array consisting of M omnidirectional microphones, where the interelement spacing is equal to δ. The steering vector as a function of the azimuthal angle, θ, is given by

$$\mathbf{d}(\omega,\theta) = \begin{bmatrix} 1 & e^{-\jmath\omega\tau_0\cos\theta} & \cdots & e^{-\jmath(M-1)\omega\tau_0\cos\theta} \end{bmatrix}^T, \quad (1)$$

where the superscript ^{T} is the transpose operator, $\jmath$ is the imaginary unit with $\jmath^2 = -1$, $\omega = 2\pi f$ is the angular frequency, $f > 0$ is the temporal frequency, and $\tau_0 = \delta/c$ is the sound propagation delay between two successive sensors at the angle $\theta = 0$.

In this study, we consider DMAs with small values of δ and the application scenario where the source of interest is from the angle $\theta = 0$ (the main lobe of the differential beamformers will also be at this angle). Then the mth microphone signal is given by

$$Y_m(\omega) = e^{-\jmath(m-1)\omega\tau_0} X(\omega) + V_m(\omega), \; m = 1, 2, \ldots, M, \quad (2)$$

where $X(\omega)$ is the source signal (also called desired signal) and $V_m(\omega)$ is the additive noise at the mth microphone. In a vector form, we can rearrange the signal model in (2) as

$$\begin{aligned} \mathbf{y}(\omega) &= \begin{bmatrix} Y_1(\omega) & Y_2(\omega) & \cdots & Y_M(\omega) \end{bmatrix}^T \\ &= \mathbf{x}(\omega) + \mathbf{v}(\omega) \\ &= \mathbf{d}(\omega, 0) X(\omega) + \mathbf{v}(\omega), \end{aligned} \quad (3)$$

where $\mathbf{x}(\omega) = \mathbf{d}(\omega, 0) X(\omega)$, $\mathbf{d}(\omega, 0)$ is the steering vector at $\theta = 0$, and the noise signal vector, $\mathbf{v}(\omega)$, is defined similarly to $\mathbf{y}(\omega)$.

978-1-5386-8151-0/18/$31.00

Beamforming consists of estimating the desired signal, $X(\omega)$, by applying a spatial filter to the sensors' outputs [13], i.e.,

$$\begin{aligned} Z(\omega) &= \sum_{m=1}^{M} H_m^*(\omega) Y_m(\omega) \\ &= \mathbf{h}^H(\omega)\mathbf{y}(\omega) \\ &= \mathbf{h}^H(\omega)\mathbf{d}(\omega,0)X(\omega) + \mathbf{h}^H(\omega)\mathbf{v}(\omega), \end{aligned} \tag{4}$$

where $Z(\omega)$ is the estimate of $X(\omega)$,

$$\mathbf{h}(\omega) = \begin{bmatrix} H_1(\omega) & H_2(\omega) & \cdots & H_M(\omega) \end{bmatrix}^T \tag{5}$$

is a complex-valued linear filter applied to the observation signal vector, $\mathbf{y}(\omega)$, and the superscripts * and ^{H} denote complex conjugation and conjugate-transpose, respectively. To ensure that the desired signal coming from $\theta = 0$ is not distorted, the distortionless constraint is needed, i.e.,

$$\mathbf{h}^H(\omega)\mathbf{d}(\omega,0) = 1. \tag{6}$$

Now that all variables are clearly defined, we are ready to give some useful performance measures.

3. PERFORMANCE MEASURES

One of the most important measures to quantify the performance of a beamformer is the so-called beampattern or directivity pattern, which describes the sensitivity of the beamformer to a plane wave impinging on the array from the direction θ. With the beamforming formulation given in (4), the beampattern is given by [8, 13],

$$\begin{aligned} \mathcal{B}[\mathbf{h}(\omega),\theta] &= \mathbf{d}^H(\omega,\theta)\mathbf{h}(\omega) \\ &= \sum_{m=1}^{M} H_m(\omega) e^{\jmath(m-1)\omega\tau_0\cos\theta}. \end{aligned} \tag{7}$$

Sensors always have self noise and mismatch among them is also inevitable. These imperfections may significantly affect a beamformer's performance. To evaluate this effect, the so-called white noise gain (WNG) is generally used; it is defined as [8]

$$\mathcal{W}[\mathbf{h}(\omega)] = \frac{\left|\mathbf{h}^H(\omega)\mathbf{d}(\omega,0)\right|^2}{\mathbf{h}^H(\omega)\mathbf{h}(\omega)}. \tag{8}$$

Another important measure, the directivity factor (DF), which quantifies the overall directional gain of a beamformer, is defined as

$$\begin{aligned} \mathcal{D}[\mathbf{h}(\omega)] &= \frac{|\mathcal{B}[\mathbf{h}(\omega),0]|^2}{\frac{1}{2}\int_0^{\pi} |\mathcal{B}[\mathbf{h}(\omega),\theta]|^2 \sin\theta d\theta} \\ &= \frac{\left|\mathbf{h}^H(\omega)\mathbf{d}(\omega,0)\right|^2}{\mathbf{h}^H(\omega)\mathbf{\Gamma}_{\mathrm{d}}(\omega)\mathbf{h}(\omega)}, \end{aligned} \tag{9}$$

where

$$\mathbf{\Gamma}_{\mathrm{d}}(\omega) = \frac{1}{2}\int_0^{\pi} \mathbf{d}(\omega,\theta)\mathbf{d}^H(\omega,\theta)\sin\theta d\theta. \tag{10}$$

The last measure that we discuss in this section is the front-to-back ratio (FBR), which is defined as the ratio of the power of the output of the array to signals propagating from the front-half plane to the output power for signals arriving from the rear-half plane. This ratio is mathematically defined as [9]

$$\begin{aligned} \mathcal{F}[\mathbf{h}(\omega)] &= \frac{\int_0^{\pi/2} |\mathcal{B}[\mathbf{h}(\omega),\theta]|^2 \sin\theta d\theta}{\int_{\pi/2}^{\pi} |\mathcal{B}[\mathbf{h}(\omega),\theta]|^2 \sin\theta d\theta} \\ &= \frac{\mathbf{h}^H(\omega)\mathbf{\Gamma}_{\mathrm{f}}(\omega)\mathbf{h}(\omega)}{\mathbf{h}^H(\omega)\mathbf{\Gamma}_{\mathrm{b}}(\omega)\mathbf{h}(\omega)}, \end{aligned} \tag{11}$$

where

$$\mathbf{\Gamma}_{\mathrm{f}}(\omega) = \int_0^{\pi/2} \mathbf{d}(\omega,\theta)\mathbf{d}^H(\omega,\theta)\sin\theta d\theta, \tag{12}$$

$$\mathbf{\Gamma}_{\mathrm{b}}(\omega) = \int_{\pi/2}^{\pi} \mathbf{d}(\omega,\theta)\mathbf{d}^H(\omega,\theta)\sin\theta d\theta. \tag{13}$$

The above definitions of the beampattern, WNG, DF, and FBR are useful for the evaluation and derivation of any types of beamformers. Next, we approximate some of these measures in order to simplify the differential beamforming design process.

4. APPROXIMATE PERFORMANCE MEASURES

In this section, we show how to approximate the DF and the FBR.

Let $\theta_p,\ p = 1, 2, \ldots, P$ be P angles, with $\theta_1 \neq \theta_2 \neq \cdots \neq \theta_P \neq 0$, $P \geq M$, and $\theta_p \in (0, \pi]$. We propose to approximate the DF as follows:

$$\mathcal{D}_{\mathrm{a}}[\mathbf{h}(\omega)] = \frac{|\mathcal{B}[\mathbf{h}(\omega),0]|^2}{\frac{1}{\sum_{p=1}^{P} w_p}\sum_{p=1}^{P} w_p |\mathcal{B}[\mathbf{h}(\omega),\theta_p]|^2}, \tag{14}$$

where $w_p,\ p = 1, 2, \ldots, P$ $(0 < w_p \leq 1)$ are some weighting factors that may depend on the nature of the noise field. In the rest, however, to simplify the presentation, we assume that $w_p = 1,\ \forall p$. Therefore, we can express the approximate DF as

$$\mathcal{D}_{\mathrm{a}}[\mathbf{h}(\omega)] = \frac{\left|\mathbf{h}^H(\omega)\mathbf{d}(\omega,0)\right|^2}{\mathbf{h}^H(\omega)\mathbf{\Upsilon}(\omega,\theta_{1:P})\mathbf{h}(\omega)}, \tag{15}$$

where

$$\mathbf{\Upsilon}(\omega,\theta_{1:P}) = \frac{1}{P}\sum_{p=1}^{P} \mathbf{d}(\omega,\theta_p)\mathbf{d}^H(\omega,\theta_p) \tag{16}$$

is an $M \times M$ matrix. We assume that $P \geq M$ so that $\mathbf{\Upsilon}(\omega,\theta_{1:P})$ has full-rank.

Let $\theta_i,\ i = 1, 2, \ldots, P_{\mathrm{f}}$ be P_{f} angles from the front-half plane, with $\theta_1 \neq \theta_2 \neq \cdots \neq \theta_{P_{\mathrm{f}}} \neq 0$ and $\theta_i \in (0, \pi/2]$, and let $\theta_j,\ j = 1, 2, \ldots, P_{\mathrm{b}}$ be P_{b} angles from the rear-half plane, with $\theta_1 \neq \theta_2 \neq \cdots \neq \theta_{P_{\mathrm{b}}}$, $P_{\mathrm{b}} \geq M$, and $\theta_j \in (\pi/2, \pi]$. In the same way as we approximated the DF, we can approximate the FBR as

$$\mathcal{F}_{\mathrm{a}}[\mathbf{h}(\omega)] = \frac{\frac{1}{\sum_{i=1}^{P_{\mathrm{f}}} w_i}\sum_{i=1}^{P_{\mathrm{f}}} w_i |\mathcal{B}[\mathbf{h}(\omega),\theta_i]|^2}{\frac{1}{\sum_{j=1}^{P_{\mathrm{b}}} w_j}\sum_{j=1}^{P_{\mathrm{b}}} w_j |\mathcal{B}[\mathbf{h}(\omega),\theta_j]|^2}. \tag{17}$$

Again, it is assumed that $w_i = w_j = 1,\ \forall i, j$, so that the approximate FBR can be rewritten as

$$\mathcal{F}_{\mathrm{a}}\left[\mathbf{h}\left(\omega\right)\right] = \frac{\mathbf{h}^H\left(\omega\right)\boldsymbol{\Upsilon}\left(\omega, \theta_{1:P_{\mathrm{f}}}\right)\mathbf{h}\left(\omega\right)}{\mathbf{h}^H\left(\omega\right)\boldsymbol{\Upsilon}\left(\omega, \theta_{1:P_{\mathrm{b}}}\right)\mathbf{h}\left(\omega\right)}, \tag{18}$$

where

$$\boldsymbol{\Upsilon}\left(\omega, \theta_{1:P_{\mathrm{f}}}\right) = \frac{1}{P_{\mathrm{f}}}\sum_{i=1}^{P_{\mathrm{f}}}\mathbf{d}\left(\omega, \theta_i\right)\mathbf{d}^H\left(\omega, \theta_i\right), \tag{19}$$

$$\boldsymbol{\Upsilon}\left(\omega, \theta_{1:P_{\mathrm{b}}}\right) = \frac{1}{P_{\mathrm{b}}}\sum_{j=1}^{P_{\mathrm{b}}}\mathbf{d}\left(\omega, \theta_j\right)\mathbf{d}^H\left(\omega, \theta_j\right). \tag{20}$$

The $M \times M$ matrix $\boldsymbol{\Upsilon}\left(\omega, \theta_{1:P_{\mathrm{f}}}\right)$ may not be full rank since we do not assume that P_{f} is greater than the number of microphones; however, the $M \times M$ matrix $\boldsymbol{\Upsilon}\left(\omega, \theta_{1:P_{\mathrm{b}}}\right)$ has full rank.

5. PSEUDO DIFFERENTIAL BEAMFORMERS

In this section, we show how to derive different differential beamformers from the approximate DF and the approximate FBR. The prefix "pseudo-" is used for all the deduced beamformers to distinguish them from their counterparts derived from the exact performance measures.

5.1. Pseudo-Hypercardioid

It is well known that the hypercardioid of order $M-1$ is obtained by maximizing the DF. In our context, maximizing (15) is equivalent to minimizing $\mathbf{h}^H\left(\omega\right)\boldsymbol{\Upsilon}\left(\omega, \theta_{1:P}\right)\mathbf{h}\left(\omega\right)$ subject to the distortionless constraint. Mathematically, this problem is written as

$$\min_{\mathbf{h}(\omega)} \mathbf{h}^H\left(\omega\right)\boldsymbol{\Upsilon}\left(\omega, \theta_{1:P}\right)\mathbf{h}\left(\omega\right) \quad \text{subject to} \quad \mathbf{h}^H\left(\omega\right)\mathbf{d}\left(\omega, 0\right) = 1. \tag{21}$$

The solution of the above problem is the $(M-1)$th-order pseudo-hypercardioid:

$$\mathbf{h}_{\mathrm{pH}}\left(\omega\right) = \frac{\boldsymbol{\Upsilon}^{-1}\left(\omega, \theta_{1:P}\right)\mathbf{d}\left(\omega, 0\right)}{\mathbf{d}^H\left(\omega, 0\right)\boldsymbol{\Upsilon}^{-1}\left(\omega, \theta_{1:P}\right)\mathbf{d}\left(\omega, 0\right)}. \tag{22}$$

5.2. Pseudo-Supercardioid

In (18), we recognize the generalized Rayleigh quotient [14]. It is well known that this quotient is maximized with the eigenvector corresponding to the maximum eigenvalue of $\boldsymbol{\Upsilon}^{-1}\left(\omega, \theta_{1:P_{\mathrm{b}}}\right)\boldsymbol{\Upsilon}\left(\omega, \theta_{1:P_{\mathrm{f}}}\right)$. Let us denote $\lambda_1\left(\omega\right)$ this maximum eigenvalue and $\mathbf{t}_1\left(\omega\right)$ the corresponding eigenvector. Then, the pseudo-supercardioid is

$$\mathbf{h}_{\mathrm{pS}}\left(\omega\right) = \alpha\left(\omega\right)\mathbf{t}_1\left(\omega\right), \tag{23}$$

where $\alpha\left(\omega\right) \neq 0$ is an arbitrary complex number. We deduce that

$$\mathcal{F}_{\mathrm{a}}\left[\mathbf{h}_{\mathrm{pS}}\left(\omega\right)\right] = \lambda_1\left(\omega\right). \tag{24}$$

Clearly, we always have

$$\mathcal{F}_{\mathrm{a}}\left[\mathbf{h}_{\mathrm{pS}}\left(\omega\right)\right] \geq \mathcal{F}_{\mathrm{a}}\left[\mathbf{h}\left(\omega\right)\right],\ \forall \mathbf{h}\left(\omega\right). \tag{25}$$

In practice, it is important to properly choose the value of $\alpha\left(\omega\right)$. The most straightforward way to find this parameter is to use the distortionless constraint. Substituting (23) into (6), we get

$$\alpha\left(\omega\right) = \frac{1}{\mathbf{d}^H\left(\omega, 0\right)\mathbf{t}_1\left(\omega\right)}. \tag{26}$$

As a result, the pseudo-supercardioid of order $M-1$ is

$$\mathbf{h}_{\mathrm{pS}}\left(\omega\right) = \frac{\mathbf{t}_1\left(\omega\right)}{\mathbf{d}^H\left(\omega, 0\right)\mathbf{t}_1\left(\omega\right)}. \tag{27}$$

5.3. Pseudo-Cardioid

As far as we know, there is no optimality associated with the cardioid. However, one of the most well-known forms of this pattern has always a null at the angle π. Therefore, we may consider the criterion:

$$\min_{\mathbf{h}(\omega)} \mathbf{h}^H\left(\omega\right)\boldsymbol{\Upsilon}\left(\omega, \theta_{1:P}\right)\mathbf{h}\left(\omega\right) \quad \text{subject to} \quad \mathbf{h}^H\left(\omega\right)\mathbf{C}_2\left(\omega\right) = \mathbf{i}_{10}^T, \tag{28}$$

where $\mathbf{C}_2\left(\omega\right) = \left[\begin{array}{cc}\mathbf{d}\left(\omega, 0\right) & \mathbf{d}\left(\omega, \pi\right)\end{array}\right]$ and $\mathbf{i}_{10} = \left[\begin{array}{cc}1 & 0\end{array}\right]^T$. We find that the $(M-1)$th-order pseudo-cardioid is

$$\mathbf{h}_{\mathrm{pC}}\left(\omega\right) = \boldsymbol{\Upsilon}^{-1}\left(\omega, \theta_{1:P}\right)\mathbf{C}_2\left(\omega\right) \times \left[\mathbf{C}_2^H\left(\omega\right)\boldsymbol{\Upsilon}^{-1}\left(\omega, \theta_{1:P}\right)\mathbf{C}_2\left(\omega\right)\right]^{-1}\mathbf{i}_{10}. \tag{29}$$

5.4. Pseudo-Dipole

The dipole of any order has a null at the angle $\pi/2$ and a one at both the angles 0 and π. So, a possible criterion to optimize for $M \geq 3$ is

$$\min_{\mathbf{h}(\omega)} \mathbf{h}^H\left(\omega\right)\boldsymbol{\Upsilon}\left(\omega, \theta_{1:P}\right)\mathbf{h}\left(\omega\right) \quad \text{subject to} \quad \mathbf{h}^H\left(\omega\right)\mathbf{C}_3\left(\omega\right) = \mathbf{i}_{101}^T, \tag{30}$$

where $\mathbf{C}_3\left(\omega\right) = \left[\begin{array}{ccc}\mathbf{d}\left(\omega, 0\right) & \mathbf{d}\left(\omega, \pi/2\right) & \mathbf{d}\left(\omega, \pi\right)\end{array}\right]$ and $\mathbf{i}_{101} = \left[\begin{array}{ccc}1 & 0 & 1\end{array}\right]^T$. We find that the $(M-1)$th-order pseudo-dipole is

$$\mathbf{h}_{\mathrm{pD}}\left(\omega\right) = \boldsymbol{\Upsilon}^{-1}\left(\omega, \theta_{1:P}\right)\mathbf{C}_3\left(\omega\right) \cdot \left[\mathbf{C}_3^H\left(\omega\right)\boldsymbol{\Upsilon}^{-1}\left(\omega, \theta_{1:P}\right)\mathbf{C}_3\left(\omega\right)\right]^{-1}\mathbf{i}_{101}. \tag{31}$$

For $M = 2$, the filter corresponding to the second-order pseudo-dipole is simply

$$\mathbf{h}_{\mathrm{pD}}\left(\omega\right) = \mathbf{C}_2^{\prime -H}\left(\omega\right)\mathbf{i}_{10}, \tag{32}$$

where $\mathbf{C}_2'\left(\omega\right) = \left[\begin{array}{cc}\mathbf{d}\left(\omega, 0\right) & \mathbf{d}\left(\omega, \pi/2\right)\end{array}\right]$.

6. EVALUATION

We have discussed the approximate DF and FBR measures in Section 4 and how to design different pseudo differential beamformers with these two performance measures in Section 5. In this section, we briefly evaluate the beampatterns of the pseudo beamformers deduced in the previous section. Note that only beampatterns are shown here and the results of the DF and the WNG are not presented due to space limitation.

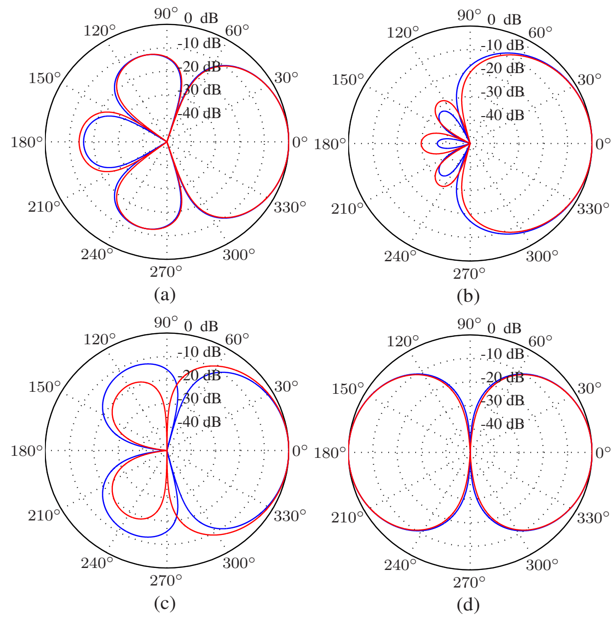

Fig. 1. Beampatterns of four 2nd-order differential beamformers at $f = 1$ kHz (—: theoretical, —: designed pseudo): (a) hypercardioid, (b) supercardioid (c) cardioid, and (d) dipole. Conditions: $M = 3$, $\delta = 1$ cm, $P = 10$, and $P_{\mathrm{f}} = P_{\mathrm{b}} = P/2$.

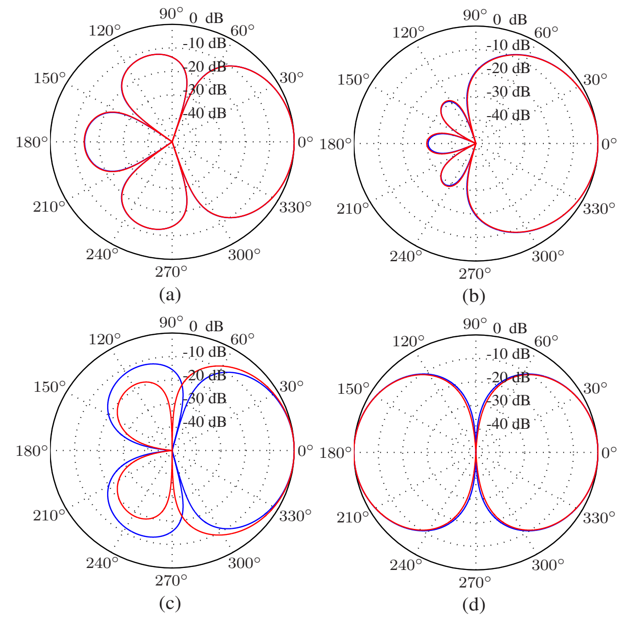

Fig. 2. Beampatterns of four 2nd-order differential beamformers at $f = 1$ kHz (—: theoretical, —: designed pseudo): (a) hypercardioid, (b) supercardioid (c) cardioid, and (d) dipole. Conditions: $M = 3$, $\delta = 1$ cm, $P = 100$, and $P_{\mathrm{f}} = P_{\mathrm{b}} = P/2$.

A uniform linear microphone array with 3 omnidirectional sensors (i.e., $M = 3$) is used and the interelement spacing, δ, is equal to 1 cm. We consider to design the 2nd-order hypercardioid, supercardioid, cardioid, and dipole beampatterns. To study the impact of the value of P on the performance, we investigate two cases: $P = 10$ and $P = 100$. In both cases, we set $P_{\mathrm{f}} = P_{\mathrm{b}} = P/2$. The beampatterns of the four designed pseudo beamformers in both situations are plotted (in blue color) in Figs. 1 and 2, respectively. For comparison, the theoretical beampatterns (from the exact definitions of the performance measures) of the four beamformers are also plotted in the figures.

From the results, we make the following observations. (1) The approximate DF and FBR measures are successful for the design of differential beamformers. The difference between the beampattens of the pseudo beamformers and the theoretical ones is small and this difference decreases with the number of total angles (i.e., the value of P) used in the approximation. (2) For the beamformers that have optimality, the beampatterns of the designed beamformers are very close to their theoretical beampatterns [see Fig. 1(a) and (b) and Fig. 2(a) and (b)]. There are some small differences between the beampattens of the pseudo beamformers and the theoretical ones if the beamformers do not have an optimality associated with it [see Fig. 1(c) and Fig. 2(c)]. The underlying reason is under investigation.

The advantage of using approximate performance measures is that they can be used to design beamformers that may not be easy to find with the exact performance measures. More results will be reported soon.

7. CONCLUSIONS

The design of DMA beamformers often involves optimization of some performance measures such as the DF, FBR, WNG, etc. In this paper, we developed two approximate performance measures, i.e., the approximate DF and FBR, and showed how to design different differential beamformers using these two approximate measures. Evaluation revealed that the beampatterns designed with the approximate measures are close to the theoretical beampatterns. The advantage of these approximate performance measures is that they are easy to evaluate and can be used to design all kind of beamformers that may not be easy to find with the exact performance measures.

8. REFERENCES

[1] G. W. Elko, S. L. Gay, and J. Benesty, *Acoustic Signal Processing for Telecommunication*, Kluwer Academic Publishers, Boston, MA, 2000.

[2] G. W. Elko, J. Meyer, J. Benesty, M. M. Sondhi, and Y. Huang, *Springer Handbook of Speech Processing*, Springer-Verlag, Berlin, GermanyGermany:, 2008.

[3] J. Benesty, J. Chen, and I. Cohen, *Design of Circular Differential Microphone Arrays*, Springer-Verlag, Switzerland, 2015.

[4] J. Benesty, I. Cohen, and J. Chen, *Fundamentals of Signal Enhancement and Array Signal Processing*, Wiley-IEEE Press, Singapore, 2018.

[5] Y. Buchris, I. Cohen, and J. Benesty, "First-order differential microphone arrays from a time-domain broadband perspective," in *Proc. IEEE IWAENC*. IEEE, September 2016, pp. 1–5.

[6] L. Zhao, J. Benesty, and J. Chen, "Optimal design of directivity patterns for endfire linear microphone arrays," in *Proc. IEEE ICASSP*. IEEE, April 2015, pp. 295–299.

[7] C. Li, J. Benesty, G. Huang, and J. Chen, "Subspace superdirective beamformers based on joint diagonalization," in *Proc. IEEE ICASSP*. IEEE, March 2016, pp. 400–404.

[8] J. Benesty and J. Chen, *Study and Design of Differential Microphone Arrays*, Springer-Verlag, Berlin, Germany, 2012.

[9] R. N. Marshall and W. R. Harry, "A new microphone providing uniform directivity over an extended frequency range," *J. Acoust. Soc.Am.*, vol. 12, pp. 481–497, April 1941.

[10] J. Chen, J. Benesty, and C. Pan, "On the design and implementation of linear differential microphone arrays," *J. Acoust. Soc. Am.*, vol. 136, pp. 3097–3113, December 2014.

[11] C. Pan, J. Chen, and J. Benesty, "Theoretical analysis of differential microphone array beamforming and an improved solution," *IEEE Trans. Audio, Speech, Lang. Process.*, vol. 23, no. 2093-2105, August 2015.

[12] T. D. Abhayapala and A. Gupta, "Higher order differential-integral microphone arrays," *J. Acoust. Soc.Am.*, vol. 127, pp. 227–233, May 2010.

[13] J. Benesty, J. Chen, and Y. Huang, *Microphone Array Processing*, Springer-Verlag, Berlin, Germany, 2008.

[14] G. H. Golub and C. F. Van Loan, *Matrix Computations*, The Johns Hopkins University Press, Baltimore, Maryland:, 1996.